

pubs.acs.org/JPCA Article

# The Effect of Methylation on the Triplet-State Dynamics of 2-Thiouracil: Time-Resolved Photoelectron Spectroscopy of 2-Thiothymine

Published as part of The Journal of Physical Chemistry virtual special issue "Paul L. Houston Festschrift". Susanne Ullrich,\* Yingqi Qu, Abed Mohamadzade, and Sarita Shrestha



Cite This: J. Phys. Chem. A 2022, 126, 8211-8217



**Read Online** 

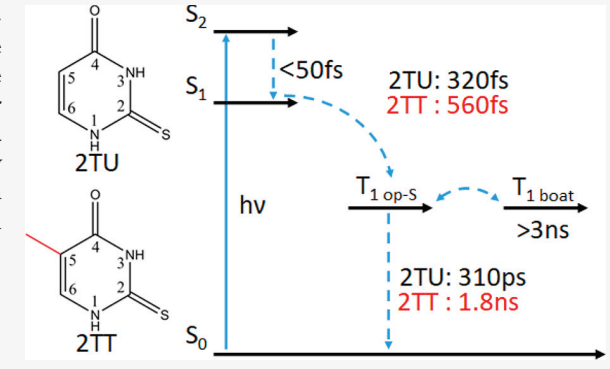
**ACCESS** 

Metrics & More

Article Recommendations

supporting Information

**ABSTRACT:** The ultrafast internal conversion and intersystem crossing dynamics of 2-thiouracil (2TU) and 2-thiothymine (2TT) are studied using time-resolved photoelectron spectroscopy to investigate the effect of methylation on the deactivation mechanism. Like other thiobases, the triplet manifold is populated with high quantum yields via the lowest singlet excited state, which is dark in absorption. This study focuses on the lowest triplet state and the role of two minima, with sulfur-out-of-plane and slightly boat-like geometries, in the intersystem crossing dynamics back to the ground state.



#### 1. INTRODUCTION

Structurally modified nucleobases such as thiobases, where an oxygen atom is replaced by sulfur, have been observed to undergo fast and efficient intersystem crossing dynamics (ISC), which populates the lowest triplet excited state,  $T_1$ , with a near-unity quantum yield. 1-4 Thiouracil derivatives follow a general pathway that involves internal conversion (IC) from an initially photoexcited singlet excited state of  ${}^1\pi\pi^*$ character, e.g.,  $S_2$  ( $\pi_S \pi_6^*$ ), to the lowest singlet excited state,  $S_1(n_S\pi_2^*)$ , which is dark in absorption. A  $^1n\pi^*/^3\pi\pi^*$  crossing point close to the S<sub>1</sub> minimum in conjunction with high spinorbit coupling (SOC) promotes ISC into the triplet manifold. An alternative pathway for ISC directly from  $S_2$  ( $\pi_S \pi_6^*$ ) has also been proposed, but it has to compete with efficient IC to  $S_1 (n_S \pi_2^*)$ . The subsequent triplet-state dynamics are sensitive to the position and degree of thionation, which profoundly alter the potential energy surface topography and SOC at the crossing point with the ground state (GS).6 Specifically, ab initio calculations revealed the presence of two triplet-state minima with boat-like ( $T_{1\ boat}$ ) and sulfur-out-of-plane ( $T_{1\ op-S}$ ) geometries.<sup>7-9</sup> The triplet-state dynamics are therefore governed by factors such as the relative energies of the minima, the barrier height separating them, and the accessibility of  $T_1/GS$  crossing points from each minimum. According to Mai et al.,  $^9$   $T_{1~\rm op\text{--}S}$  and  $T_{1~\rm boat}$  are associated with different orbital transitions,  $\pi_S \rightarrow \pi_2^*$  and  $\pi_5 \rightarrow \pi_6^*$ , respectively; these transitions use the labeling scheme defined in ref 8, with the subscript indicating the primary orbital

localization. The relative energies of the minima are determined by two distinct factors that result in delocalization and, consequently, energetic stabilization: (1) conjugation between the C4=X (X = S, O) and C5=C6 bonds stabilizes  $\pi_5$  and  $\pi_6^*$  orbital transitions relative to  $\pi_5$  and  $\pi_2^*$  and (2) electrons along C=S bonds are more delocalized than those along C=O bonds due to the larger size of the sulfur atom. Consequently, these seemingly minor single-atom changes in the series of thionated uracils and thymines can profoundly alter the UV photodynamics of these compounds. In the case of 2-thionation, these effects cause a double-well potential with energetically similar  $T_{1 \text{ boat}}$  and  $T_{1 \text{ op-S}}$  minima. In contrast, 4and 2,4-thionation substantially increase the energy gap, leading to a triplet potential with effectively one single minimum, i.e.,  $T_{1 \text{ boat}}$ . Furthermore, the  $T_1$  electronic character and coordinate promoting ISC to and from T1 are affected by the substituent position. 10 This was reflected in experimental TRPES studies on a series of thiouracils, 11-14 which demonstrated tens to hundreds of picoseconds ISC from T<sub>1</sub> op-S back to the ground state in the case of 2-thiouracil (2TU);

Received: August 24, 2022 Revised: October 1, 2022 Published: November 1, 2022





in contrast, 4-thiouracil (4TU) and 2,4-dithiouracil (DTU) are subject to nanosecond trapping on the lowest triplet state, i.e.,  $T_{1\ boat}$ . Barbatti et al.<sup>7</sup> extended the idea to other thiobase derivatives and proposed a more general two-step mechanistic model with rate-determining steps of either a slow barrier crossing between the two minima or fast ISC to the GS.

While the photophysics of the thiobases in the solution phase have been studied extensively, 1,2,4,15 gas-phase experiments to date have primarily focused on thiouracils. 12-14 These studies indicate significant differences between the solution-phase and gas-phase triplet-state dynamics. 12,16 In solution, the two T<sub>1</sub> minima are nondegenerate due to a stabilization of  $T_{1\,boat}$  with respect to  $T_{1\,op\text{-S}}$ , although this was recently questioned by experimental evidence for a  $T_1$  doublewell potential consistent with the gas phase. 15 The TRPES study presented here extends the earlier gas-phase work to thiothymine and further interrogates the double-well topography of the triplet state associated with the 2-thionation of uracil and thymine. According to ab initio calculations and dynamics simulations, 8,9,17 the minimum-energy pathway starts from a near planar  $S_2$  ( $\pi_S \pi_6^*$ ) geometry and proceeds along a coordinate that maintains a mostly planar ring but with increasing out-of-plane displacement of the sulfur atom at the  $S_1$   $(n_S\pi_2^*)$  minimum and the initially populated  $T_1$  op-S. Methylation in 2-thiothyimne (2TT) provides a sensitive probe of the deactivation coordinates and barriers along the pathway, which involves the displacement of the methyl substituent and will manifest itself in slower triplet dynamics. As such, it offers insight into the role of the boat-like  $T_1$ minimum and mechanisms mediated by a ring-puckering coordinate.

#### 2. EXPERIMENTAL AND COMPUTATIONAL DETAILS

The time-resolved photoelectron spectroscopy (TRPES) apparatus consists of a Coherent Inc. Legend Elite HE amplified ultrafast laser system with two tunable optical parametric amplifiers, TOPAS and OPerA, and a magnetic bottle photoelectron spectrometer, which has been described in detail elsewhere. <sup>18,19</sup>

The 2-thiothymine (AK Scientific, purity 98%) and 2thiouracil (Sigma-Aldrich, purity 99%) sample powders were heated in a quartz sample holder to 180 and 205 °C, respectively, and coexpanded with a He carrier gas through a pinhole nozzle. The resulting continuous molecular beam was doubly skimmed before it entered the ionization region of the magnetic bottle, where it intersected with the pump and timedelayed probe pulses. Pump pulses of 303 nm were derived from the OperA to photoexcite the molecules on the emergence of their first absorption band. To reduce undesirable probe-pump signals, the TOPAS was tuned to a probe wavelength of 330 nm below the absorption onset. The pump  $(1.3-1.4 \mu I)$  and probe  $(4.8-5.5 \mu I)$  beams were focused by two separate 50 cm lenses and spatially overlapped at a small angle. The molecules undergo a 1 + 2' excitationionization process, and photoelectron kinetic energies were recorded at different pump-probe delays to acquire a timeresolved photoelectron spectrum. To facilitate easy comparison with ab initio-calculated ionization energies, the photoelectron spectra were plotted as a function of electron binding energy (eBE), i.e., the measured electron kinetic energies subtracted from the total (1 + 2') photon energy. TRPES spectra were recorded with an unequal and increasing step size over an

extended pump—probe delay range of 3 ns, which was enabled by an Ultrafast Systems Smart Delay Line.

Timing and energy calibrations were conducted through TRPES measurements of a 50:50 1,3-butadiene and He mixture. A Gaussian cross-correlation function describes the instrument response function, with a full width at half-maximum of around 200 fs. Energy calibrations use known ionization potentials and vibrational features of 1,3-butadiene to convert electron time-of-flight measurements to kinetic energies.

The experimental TRPES spectra of 2TT and 2TU were analyzed using Glotaran<sup>21</sup> to extract evolution-associated spectra (EAS) and their time constants. The experimental data was then interpreted with the aid of ab initio calculations, specifically the excited-state deactivation pathway and ionization energies at critical points along the path. For 2TU, this information is available from the CASPT2 calculations in ref 11. For 2TT, DFT-based calculations were performed in ORCA 5<sup>22</sup> at the CAM-B3LYP def2-TZVP level of theory. The geometries of the neutral ground and excited states were optimized, and excitation energies were obtained. For each optimized geometry, vertical ionization energies were computed with single-point energy calculations. Neutral electronic excited states of  $n\pi^*$  and  $\pi\pi^*$  character preferentially ionize into the two lowest cationic states,  $D_1(n^{-1})$  – hole and  $D_0(\pi^{-1})$ -hole, respectively. Due to the small energy difference, their photoelectron bands overlap and, for the purpose of TRPES analysis, can be considered a single ionization channel.<sup>11</sup> When predicting the eBE range of experimental photoelectron bands, changes in the ionization potential and vibrational excitation were taken into account. In addition to changes in the ionization potential along the relaxation path, electronic relaxation is also associated with vibrational energy gain. In a simple picture, it can be assumed that the vibrational excitation in the neutral excited state is transferred to the cation upon photoionization ( $\Delta v = 0$ propensity rule). This causes a shift of the photoelectron bands toward higher eBEs compared to the calculated ionization energies. This additional shift due to vibrational excitation is taken into account in the interpretation of the location and shape of the EAS (see SI Table S1).

#### 3. RESULTS AND DISCUSSION

3.1. Static Picture of 2TU and 2TT Photophysics. Figure 1 presents the experimental solution-phase UV-vis spectra of 2TU and 2TT in ethanol (EtOH) from refs 23 and 16. The uracil (U) spectrum is also shown for comparison. Gas-phase UV-vis spectra are only available for U and 2TU and show features similar to the spectra recorded in EtOH. 16,23,24 Based on this comparison, the 2TT UV-vis spectrum in EtOH is also expected to resemble the one in the gas phase. The similarity of the 2TT and 2TU absorption spectra indicates that methylation only minimally affects the electronic structures of these molecules, which might therefore share the same general deactivation mechanism visualized in Figure 2. Two bright singlet excited states, i.e.,  $S_4$  ( $\pi_S \pi_2^*$ ) and  $S_2$  ( $\pi_S \pi_6^*$ ), contribute to the first absorption band spanning from 325 (3.8 eV) to 250 nm, while the  $S_1$  ( $n_S\pi_2^*$ ) state is dark in the absorption spectrum due to the negligible oscillator strength. The onsets of the 2TT and 2TU experimental absorption spectra coincide with each other, indicating similar adiabatic excitation energies from the ground state to the S<sub>2</sub>  $(\pi_S \pi_6^*)$  minimum. For 2TU, the  $S_2$   $(\pi_S \pi_6^*)$  minimum energy

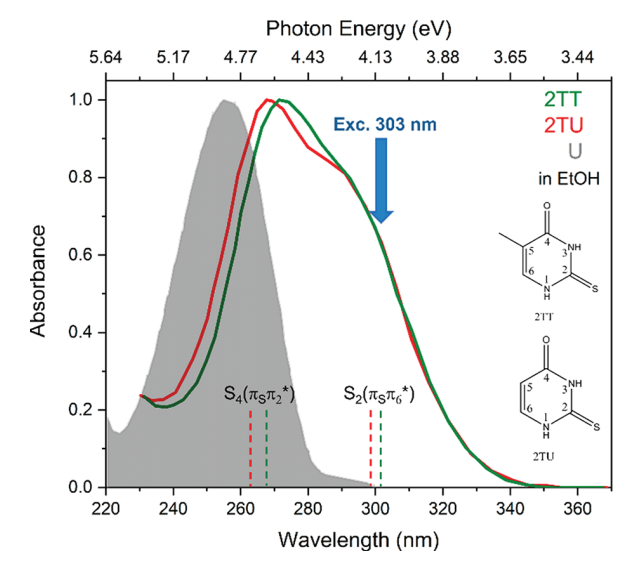


**Figure 1.** Experimental solution-phase UV-vis absorption spectra of 2TU (red) and 2TT (green) in EtOH; for comparison, the uracil spectrum is shown as a gray shaded area. The two bright  $\pi_S \to \pi^*$  transitions contributing to the first absorption band of both thiobases are indicated with dashed lines, and the excitation wavelength used in the TRPES measurements is represented by a blue arrow. The molecular structures with atomic numbering are also shown as insets.

is known from ab initio calculations and amounts to 3.75 eV. Therefore, initial photoexcitation with a 303 nm (4.1 eV) pump populates  $S_2$  ( $\pi_S \pi_6^*$ ) with an excess vibrational energy of  $\sim$ 0.3 eV.

A theory-guided model of the photophysical pathway and knowledge of critical points on the potential energy surfaces are beneficial for interpreting the TRPES to extract the underlying photodynamic mechanism. The model, based on extensive computational work, <sup>7-10</sup> is visualized in Figure 2, and relevant parameters of the potential energy surfaces are summarized in Table 1. Evolution along the minimum-energy pathway involves sequential IC and ISC processes from planar S<sub>2</sub> ( $\pi_8\pi_6^*$ ) to S<sub>1</sub>( $n_8\pi_2^*$ ) and from S<sub>1</sub>( $n_8\pi_2^*$ ) to T<sub>1</sub> via T<sub>2</sub>, respectively, along a sulfur-out-of-plane coordinate. Once the T<sub>1 op-S</sub> minimum located at 2.96 eV for 2TU and 3.2 eV for 2TT is reached, the vibrational excitation amounts to ~1.1 and ~0.9 eV, respectively. This provides sufficient energy to access the crossing point back to the ground state or alternatively to surmount the barrier to the almost isoenergetic T<sub>1 boat</sub>

minimum. Intersystem crossing occurs along an increasing sulfur-out-of-plane distortion and is facilitated by high spin—orbit coupling at a  $T_{1 \text{ opt-S}}/GS$  crossing point located 0.2-0.3 eV above the minimum. In the latter case, a decrease in the op-S angle combined with very slight ring puckering leads over the barrier (2TU, 0.1 eV; 2TT, 0.2 eV) to  $T_{1 \text{ boat}}$  but intersystem crossing to the GS from this minimum is disfavored due to low SOC. Furthermore, the  $T_{1 \text{ boat}}/GS$  crossing point is slightly higher in energy, and accessing it requires the significant molecular distortion of the ring and the methyl group. Given the complex triplet-state topography, the fate of the  $T_{1 \text{ opt-S}}$  population requires an evaluation from a dynamics perspective, which is the focus of the TRPES analysis and discussion presented below.

3.2. Time-Resolved Photoelectron Spectra of 2TU and 2TT Photodynamics. Figure 3 shows the TRPES spectra of 2TU (left) and 2TT (right) following photoexcitation to their optically bright singlet excited state of  $\pi\pi^*$ character, i.e.,  $S_2(\pi_S \pi_6^*)$ . Photoelectron kinetic energy spectra were recorded at various pump-probe delays and plotted in the colormaps in terms of electron binding energies. The dots superimposed on the colormaps indicate the energy range in which a photoelectron band associated with ionization from a particular excited state is expected. These estimates are based on ab initio calculations described in the experimental section, and the values are listed in SI Table S1. The TRPES spectrum of 2TT closely resembles that of 2TU, implying that both share the same general deactivation mechanism. Furthermore, the overall agreement between theoretical and observed shifts in the photoelectron spectra as a result of IC and ISC confirms the relaxation along the minimum-energy pathway predicted by ab initio calculations. The TRPES spectra were processed using target analysis techniques based on a sequential decay model for a more quantitative assessment. Four exponential decay components were necessary to adequately describe the data, and evolution-associated spectra were extracted for further interpretation and discussion.

**3.3. 2-Thiouracil.** The gas-phase photodynamics of 2TU were studied recently 11,12,25 using TRPES combined with ab initio calculations, which established a good understanding of the mechanistic details leading to the efficient population of the triplet manifold. However, in this earlier work the observation window was limited to 300 ps, which was insufficient to, at least partially, capture the slower triplet-state dynamics. The present study shows general agreement and confirms the previous observations and interpretation of

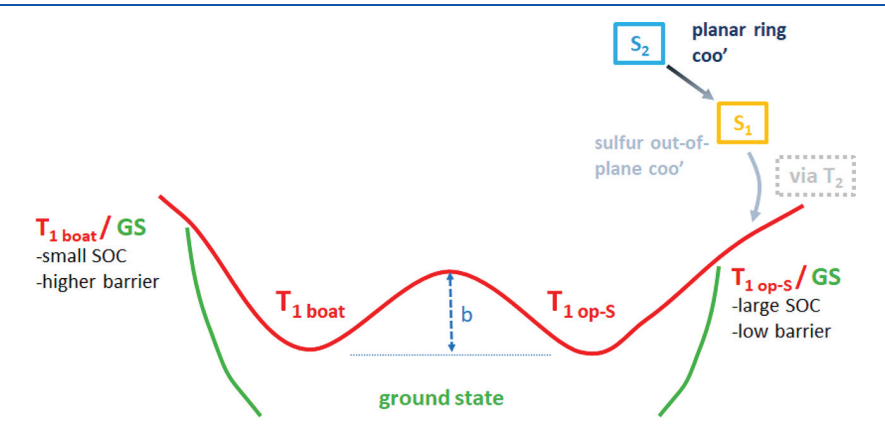


Figure 2. Schematic of the deactivation pathway of 2TU and 2TT. Energies of the critical points and barriers are summarized in Table 1.

Table 1. Critical Points and Characteristics of the 2TU and 2TT Excited-State Potential Energy Surfaces<sup>a</sup>

	2TU <sup>8,11</sup>	$2\mathrm{TT}^7$
	MS-CASPT2(12,9)/cc-pVDZ	MS-CASPT2(10,7)/ANO-RCC-VTZP
S <sub>2</sub> min (eV)	3.75	
$S_2/S_1$ CI (eV)	3.79	
$S_1 \min (eV)$	3.33	
$S_1/T_2$ (eV)	3.42	
$T_{1 \text{ op-S}} \min (eV)$	2.96	3.2
$T_{1 \text{ boat}} \min (eV)$	2.96	3.23
barrier $b$ (eV)	0.1	0.2
$T_{1 \text{ op-S}}/GS \text{ (eV)}$	3.16	3.5
$SOC T_{1 \text{ op-S}}/GS \text{ (cm}^{-1})$	150	79
$T_{1 \text{ boat}}/G\hat{S} \text{ (eV)}$	3.38	4.1
SOC $T_{1 \text{ boat}}/GS \text{ (cm}^{-1})$	2	~0

"Energies of excited-state minima, crossing points, the triplet-state barrier height (b), and the spin-orbit coupling constants (SOC) were obtained from computational studies in the literature.

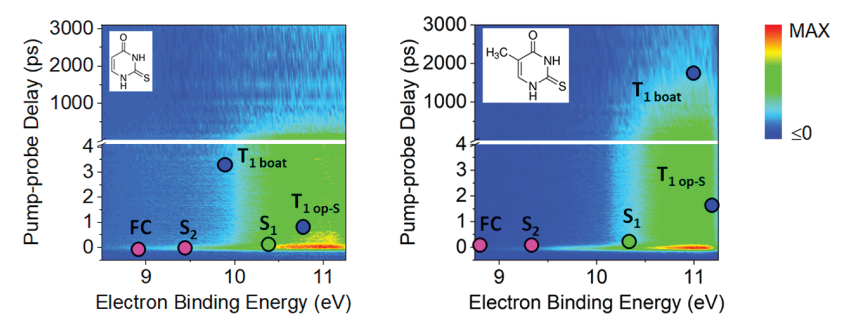


Figure 3. Experimental TRPES of 2TU (left) and 2TT (right). The dots superimposed on the colormaps indicate the electron binding energy range in which photoelectron bands are expected to appear for ionization from the  $S_2$  ( $\pi_5\pi_6^*$ ) Franck—Condon region (FC) and minimum ( $S_2$ ), the  $S_1$  ( $n_5\pi_2^*$ ) minimum ( $S_1$ ), and the two triplet minima ( $S_1$ ). Values were derived from ab initio calculations and are listed in SI Table S1.

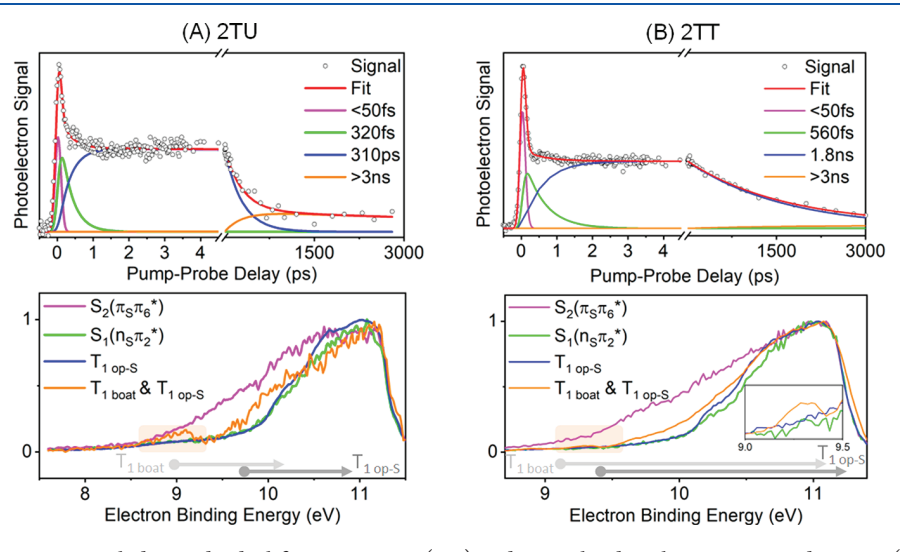


Figure 4. Integrated time traces, including individual fit components (top) and normalized evolution-associated spectra (bottom), of 2TU (left) and 2TT (right). The arrows below the evolution-associated spectra indicate the electron binding energy range in which photoelectron bands for ionization from the  $T_{1 \text{ boat}}$  and  $T_{1 \text{ op-S}}$  minima are expected. The dot of the arrow is located at the vertical ionization energy, whereas the tip includes the maximum amount of vibrational excitation that can be transferred to the cation upon photoionization (see SI Table S1). The error for the provided time constants was estimated as ~20% based on fitting statistics.

the femto- and picosecond dynamics. With the extension of the pump-probe range to 3 ns, a long-lived component becomes clearly apparent, which necessitates the inclusion of a fourth exponential decay component (see Figure 4A, top). As a consequence of the modified fit equation, time constants extracted from the global lifetime analysis differ from previous

time constants slightly more than the reported errors of ~20%. However, the derived photophysical model for the femtosecond and picosecond IC and ISC dynamics remains unchanged. Specifically, the first step involves relaxation from the FC region of the  $S_2$  ( $\pi_S\pi_6^*$ ) state and ultrafast (<50 fs) internal conversion to the  $S_1$  ( $n_S\pi_2^*$ ) state. Subsequent ISC via

a crossing point with a sizable SOC of 130 cm<sup>-1</sup> in the vicinity of the state minimum<sup>8,9</sup> populates the lowest triplet state  $T_1$  $(\pi\pi^*)$  on a time scale of 320 fs. According to ab initio calculations (SI Table S1), a very significant (~1.34 eV) shift in the photoelectron spectrum toward higher eBE is likely due to the increase in the ionization potential and the excited state vibrational energy gain during the  $S_2 \rightarrow S_1 \rightarrow T_1$  relaxation process. This shift is clearly visible in the TRPES colormap in Figure 3, left, in agreement with the superimposed dots that represent the ab initio predictions. Furthermore, this is also reflected in the evolution-associated spectra of the <50 and 310 fs decay (pink  $(S_2)$  and green  $(S_1)$  curves in Figure 4A, bottom, respectively), with onsets around 8.5 and 9.75 eV. The small (0.2 eV) spectral shift associated with  $S_1 \rightarrow T_1$ intersystem crossing is less apparent in the TRPES colormap due to the inherently broad nature of time-resolved photoelectron spectra. However, spectral changes in the two evolution-associated spectra attributed to T<sub>1</sub> (blue and orange curve) hint at intriguing triplet-state dynamics on longer time scales beyond hundreds of picoseconds. The blue evolutionassociated spectrum falls within the eBE range (indicated by a dark gray arrow) assigned to ionization from the  $T_{1 \text{ op-S}}$ minimum. Therefore, this confirms trajectory simulations that predict ISC from the sulfur-out-of-plane (op-S) geometry of the  $S_1$  minimum to  $T_{1 \text{ op-}S}$  along a coordinate with an increasing sulfur angle. The T<sub>1 op-S</sub> spectrum decays within 310 ps, but several pathways might contribute to the depopulation of this minimum. For example, ISC back to the ground state is possible by continuing along the op-S coordinate to a crossing point 0.2 eV above the  $T_{1 \text{ op-S}}$  minimum.<sup>12</sup> The transition is promoted by a high SOC constant (150 cm<sup>-1</sup>) and an Swagging motion that modulates the singlet-triplet energy gap. Given the double-well potential of the triplet state and the relatively low barrier of 0.1 eV, interconversion from the  $T_{1 \text{ op-S}}$ min to the  $T_{1 \text{ boat}}$  minimum is another likely option. On the longer time scales that govern the T<sub>1</sub> dynamics, the molecular system, through vibrational energy transfer and barrier crossing, equilibrates and loses the memory of the op-S relaxation coordinate that initially led to the population of the triplet manifold. As vibrational energy redistributes into other degrees of freedom, broadening and shifting the photoelectron band toward lower eBE is expected, which is clearly visible for the dominant  $T_{1 \text{ op-S}}$  feature in the orange EAS. Comparing the blue and orange ÉAS in Figure 4A, bottom, the appearance of an additional small feature at nanosecond delays provides evidence of population equilibration. The gray arrows with the dot and tip, respectively, indicate zero and maximum transfer of vibrational excitation to the cation upon photoionization. The feature aligns well with the expected eBE range (indicated by a light gray arrow) for ionization from the slightly boat-like geometry of the  $T_{1\, boat}$  minimum. An equilibration ratio of 2:1 between the  $T_{1 \text{ opt-S}}$  and  $T_{1 \text{ boat}}$  minima in favor of the  $T_{1 \text{ opt-S}}$ minimum has been predicted based on trajectory simulations. Depopulation of the  $T_{1 \text{ boat}}$  minimum occurs on time scales longer than the experimental window. Nevertheless, spectral features in the orange EAS captured within the 3 ns time range provide hints as to the deactivation mechanism. The low SOC constant of 2 cm<sup>-1</sup>, pronounced molecular distortion, and high energy of the  $T_{1 \text{ boat}}/GS$  crossing point render ISC back to  $S_0$ less likely, 12 and alternative routes such as radiative decay or interconversion back to the  $T_{1 \text{ op-S}}$  minimum must also be considered. Solution-phase and matrix studies have demonstrated phosphorescence with high quantum yields on time

scales up to milliseconds. <sup>16</sup> Whether this route is also active in the absence of vibrational energy quenching to the solvent remains an open question. Therefore, possible explanations for the nanosecond dynamics include radiative decay (phosphorescence), reverse barrier crossing to access the  $T_{1 \text{ op-S}}$  pathway, or direct ISC at the  $T_{1 \text{ boat}}/GS$  crossing point. While none of these options can be excluded with any certainty, the significant presence of a  $T_{1 \text{ op-S}}$  feature in the orange EAS indicates that the  $T_{1 \text{ op-S}}$  minimum and the  $T_{1 \text{ op-S}}/GS$  crossing continue to play a role in the slower triplet-state dynamics beyond 3 ns.

**3.4. 2-Thiothymine.** Analogous to the 2TU photophysics, 2TT is expected to internally convert from the photoexcited planar  $S_2$  ( $\pi_S \pi_6^*$ ) to the sulfur-out-of-plane  $S_1$  ( $n_S \pi_2^*$ ) minimum, and subsequent intersystem crossing to the T<sub>1</sub>  $(\pi\pi^*)$  triplet is mediated by the same coordinate. Again, there is good agreement between the predicted and observed shifts in the photoelectron spectra, as visualized by the dots superimposed onto the TRPES colormap in Figure 3, right. These first two steps occur on time scales of <50 and 560 fs, respectively, according to the decay dynamics in Figure 4B, top, extracted through global lifetime analysis. The  $S_2 \rightarrow T_1$ evolution is again accompanied by an initial large (1.84 eV) shift of the photoelectron band toward higher eBE and is clearly visible in the TRPES colormap and the pink, green, and blue evolution-associated spectra. The ISC time constant, which is associated with the population of the  $T_{1 \text{ op-S}}$ minimum, is only slightly longer than that in 2TU. This is not surprising given that the methyl group is positioned across the ring from the sulfur substituent and minimally affects the highly localized sulfur-out-of-plane transition coordinate. However, noticeable differences were observed in the subsequent triplet-state dynamics upon methylation; for example, ISC crossing from the  $T_{1 \text{ op-S}}$  minimum back to  $S_0$ is almost six times slower than that in 2TU. The blue time trace components in Figure 4, top, correspond to 1.8 ns and 310 ps exponential decay constants for 2TT and 2TU, respectively. According to ab initio calculations, two factors might contribute to this. The T<sub>1 op-S</sub>/GS crossing point is higher in energy by 0.1 eV for 2TT, and the SOC decreases significantly from 150 cm<sup>-1</sup> for 2TU to 79 cm<sup>-1</sup> for 2TT (see Table 1). The signal does not decay back to zero over the 3 ns experimental observation window, and the inclusion of a fourth time constant improves the fit at long pump-probe delays. This fit component is shown in orange in Figure 4B and contributes a small increasing signal to the integrated time trace fit and an EAS that almost resembles the 1.8 ns one shown in blue. The dominant photoelectron band at 10-11.5 eV is the remaining population in  $T_{1 \text{ op-S}}$ . However, closer inspection of the lower eBE region around 9-9.5 eV (see inset) indicates the presence of a tiny feature similar to the one assigned to ionization from  $T_{1 \text{ boat}}$  in 2TU. Again, the locations of both photoelectron signals are in good agreement with the predictions shown as gray arrows. It should be noted that the predictions for 2TT are based on DFT methods (SI Table S1), which are not as accurate as the CASPT2 calculations for 2TU. As shown by ref 7, high-level correlated methods are required to precisely describe the relative energies of the two T<sub>1</sub> minima. While an equilibration ratio of 3:1 for the  $T_{1 \text{ boat}}/T_{1}$ op-S populations is expected based on theory, the limited observation window only provides a first glimpse of the increasing  $T_{1 \text{ boat}}$  population. It can be assumed that the  $T_{1 \text{ boat}}$ population decays at even longer delays via a similar mechanism as 2TU. In the solution phase, radiative decay via phosphorescence with a high quantum yield has been reported, <sup>16</sup> interestingly in a wavelength range with a significant redshift and on longer time scales compared to 2TU. Whether this shift is intrinsic to the molecule, i.e., the relative alignment of the triplet- and ground-state potential energy surfaces, or altered solvent effects by methylation has not been investigated. Therefore, it is unknown whether this is relevant and applicable to the gas phase.

#### 4. CONCLUSIONS

This TRPES study presents the first measurements of the photophysics of 2TT in the gas phase and, through comparison to 2TU, provides insight into the dynamics of the lowest triplet state,  $T_1$ , of both molecules. Figure 5 visualizes the

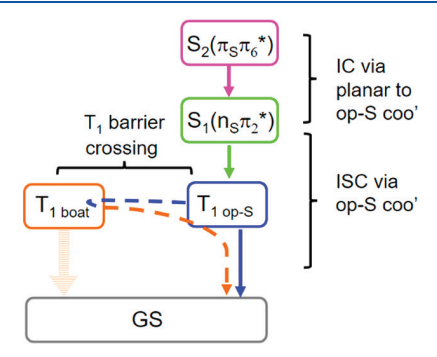


**Figure 5.** Photophysical model for 2TU and 2TT. The mechanism involves internal conversion (IC) and intersystem crossing (ISC) via  $T_{1 \text{ op-S}}$ , equilibration between  $T_{1 \text{ op-S}}$  and  $T_{1 \text{ boat}}$  via barrier crossing and vibrational energy redistribution, and  $T_{1 \text{ boat}}$  depopulation by reverse barrier crossing back to  $T_{1 \text{ op-S}}$ . Direct pathways from  $T_{1 \text{ boat}}$  to GS (larger orange arrow) facilitated by phosphorescence or ISC through a  $_{T1 \text{ boat/GS}}$  crossing point cannot be excluded.

photophysical model for gas-phase 2TU and 2TT proposed based on the TRPES results in combination with ab initio calculations. The photoexcited  $S_2$  ( $\pi_S \pi_6^*$ ) state internally converts in less than 50 fs to the lowest singlet state, S<sub>1</sub>  $(n_S\pi_2^*)$ , along a coordinate that leads to a sulfur-out-of-plane displacement. The same coordinate promotes efficient ISC into the lowest triplet state of  $\pi\pi^*$  character, constituting a double-well potential. The minima are characterized by a sulfur-out-of-plane geometry, T<sub>1 op-S</sub>, and a slightly boat-like ring distortion,  $T_{1 \text{ boat}}$ . It is the  $T_{1 \text{ op-S}}$  minimum that is initially populated via ISC (320 fs for 2TU and 560 fs for 2TT) from the  $S_1$  ( $n_S\pi_2^*$ ) state. A low barrier to a  $T_{1 \text{ op-S}}/GS$  crossing point and high SOC coupling promote ISC back to the ground state within 310 ps or 1.8 ns in the case of 2TU or 2TT, respectively. On a time scale of hundreds of pico- and nanoseconds, the system also equilibrates between the two T<sub>1</sub> minima through vibrational energy transfer and barrier crossing. However, the higher energy and low SOC of the T<sub>1 boat</sub>/GS crossing makes ISC back to the ground state less favorable. Instead, the T<sub>1 boat</sub> minimum might depopulate by phosphoresces or via barrier crossing back to  $T_{\rm 1\ opt\text{-}S}$  to access the T<sub>1 op-S</sub>/GS crossing. In the future, gas-phase time-resolved photoionization and emission experiments over a nanosecond to millisecond time scale would be desirable to further elucidate the  $T_{1\ boat}$  deactivation mechanisms.

Overall, this study shows that the methylation in 2TT leads to slower ISC dynamics compared to that in 2TU. This is explained by changes in the triplet-state topography, such as the barrier height separating the triplet state minima and the accessibility of the  $\rm T_{1\,op\text{-}S}/GS$  and  $\rm T_{1\,boat}/GS$  crossing points. A theoretical study focused on a direct comparison of the 2TU and 2TT triplet-state dynamics would be valuable for further insights into the effect of the methyl group on the deactivation mechanism.

#### ASSOCIATED CONTENT

#### Supporting Information

The Supporting Information is available free of charge at https://pubs.acs.org/doi/10.1021/acs.jpca.2c06051.

Excitation-state energies, ionization energies, estimates of vibrational energy gain during electronic relaxation, optimized geometries for 2TT, plots of selected timetraces, and spectra from the TRPES data (PDF)

#### AUTHOR INFORMATION

#### **Corresponding Author**

Susanne Ullrich — Department of Physics and Astronomy, University of Georgia, Athens, Georgia 30602, United States; oorcid.org/0000-0002-1828-2777; Email: ullrich@uga.edu

#### **Authors**

Yingqi Qu — Department of Physics and Astronomy, University of Georgia, Athens, Georgia 30602, United States Abed Mohamadzade — Department of Physics and Astronomy, University of Georgia, Athens, Georgia 30602, United States

Sarita Shrestha – Department of Physics and Astronomy, University of Georgia, Athens, Georgia 30602, United States

Complete contact information is available at: https://pubs.acs.org/10.1021/acs.jpca.2c06051

#### Notes

The authors declare no competing financial interest.

#### ACKNOWLEDGMENTS

This work was supported by the National Science Foundation Grants CHE-1800050, 2106353, and 2135351.

#### REFERENCES

- (1) Arslancan, S.; Martínez-Fernández, L.; Corral, I. Photophysics and Photochemistry of Canonical Nucleobases' Thioanalogs: From Quantum Mechanical Studies to Time Resolved Experiments. *Molecules* **2017**, 22 (6), 998.
- (2) Pollum, M.; Martínez-Fernández, L.; Crespo-Hernández, C. E. Photochemistry of Nucleic Acid Bases and Their Thio- and Aza-Analogues in Solution. In *Photoinduced Phenomena in Nucleic Acids I: Nucleobases in the Gas Phase and in Solvents*; Barbatti, M., Borin, A. C., Ullrich, S., Eds.; Topics in Current Chemistry, Vol. 355; Springer International Publishing, 2015; pp 245–327.
- (3) Mai, S.; Pollum, M.; Martínez-Fernández, L.; Dunn, N.; Marquetand, P.; Corral, I.; Crespo-Hernández, C. E.; González, L. The origin of efficient triplet state population in sulfur-substituted nucleobases. *Nat. Commun.* **2016**, *7* (1), 13077.
- (4) Ashwood, B.; Pollum, M.; Crespo-Hernández, C. E. Photochemical and Photodynamical Properties of Sulfur-Substituted Nucleic Acid Bases. *Photochem. Photobiol.* **2019**, 95 (1), 33–58.
- (5) Gobbo, J. P.; Borin, A. C. 2-Thiouracil deactivation pathways and triplet states population. *Computational and Theoretical Chemistry* **2014**, *1040*, 195–201.

- (6) Manae, M. A.; Hazra, A. Triplet Decay Dynamics in Sulfur-Substituted Thymine: How Position of Substitution Matters. *J. Phys. Chem. A* **2019**, *123* (51), 10862–10867.
- (7) Bai, S.; Barbatti, M. On the decay of the triplet state of thionucleobases. *Phys. Chem. Chem. Phys.* **2017**, 19 (20), 12674–12682.
- (8) Mai, S.; Marquetand, P.; González, L. A static picture of the relaxation and intersystem crossing mechanisms of photoexcited 2-thiouracil. *J. Phys. Chem. A* **2015**, *119* (36), 9524–9533.
- (9) Mai, S.; Marquetand, P.; González, L. Intersystem crossing pathways in the noncanonical nucleobase 2-thiouracil: A time-dependent picture. *journal of physical chemistry letters* **2016**, 7 (11), 1978–1983.
- (10) Bai, S.; Barbatti, M. Why replacing different oxygens of thymine with sulfur causes distinct absorption and intersystem crossing. *J. Phys. Chem. A* **2016**, 120 (32), 6342–6350.
- (11) Yu, H.; Sanchez-Rodriguez, J. A.; Pollum, M.; Crespo-Hernández, C. E.; Mai, S.; Marquetand, P.; González, L.; Ullrich, S. Internal conversion and intersystem crossing pathways in UV excited, isolated uracils and their implications in prebiotic chemistry. *Phys. Chem. Chem. Phys.* **2016**, *18* (30), 20168–20176.
- (12) Sánchez-Rodríguez, J. A.; Mohamadzade, A.; Mai, S.; Ashwood, B.; Pollum, M.; Marquetand, P.; González, L.; Crespo-Hernández, C. E.; Ullrich, S. 2-Thiouracil intersystem crossing photodynamics studied by wavelength-dependent photoelectron and transient absorption spectroscopies. *Phys. Chem. Chem. Phys.* **2017**, *19* (30), 19756–19766.
- (13) Mohamadzade, A.; Bai, S.; Barbatti, M.; Ullrich, S. Intersystem crossing dynamics in singly substituted thiouracil studied by time-resolved photoelectron spectroscopy: Micro-environmental effects due to sulfur position. *Chem. Phys.* **2018**, *515*, *572*–*579*.
- (14) Mohamadzade, A.; Ullrich, S. Internal conversion and intersystem crossing dynamics of uracil upon double thionation: a time-resolved photoelectron spectroscopy study in the gas phase. *Phys. Chem. Chem. Phys.* **2020**, 22 (27), 15608–15615.
- (15) Koyama, D.; Milner, M. J.; Orr-Ewing, A. J. Evidence for a double well in the first triplet excited state of 2-thiouracil. *J. Phys. Chem. B* **2017**, *121* (39), 9274–9280.
- (16) Vendrell-Criado, V.; Sáez, J. A.; Lhiaubet-Vallet, V.; Cuquerella, M. C.; Miranda, M. A. Photophysical properties of 5-substituted 2-thiopyrimidines. *Photochemical & Photobiological Sciences* **2013**, *12* (8), 1460–1465.
- (17) Cui, G.; Fang, W.-h. State-specific heavy-atom effect on intersystem crossing processes in 2-thiothymine: A potential photodynamic therapy photosensitizer. *J. Chem. Phys.* **2013**, 138 (4), 044315
- (18) Evans, N. L.; Ullrich, S. Wavelength dependence of electronic relaxation in isolated adenine using UV femtosecond time-resolved photoelectron spectroscopy. *J. Phys. Chem. A* **2010**, *114* (42), 11225–11230.
- (19) Godfrey, T.; Yu, H.; Ullrich, S. Investigation of electronically excited indole relaxation dynamics via photoionization and fragmentation pump-probe spectroscopy. *J. Chem. Phys.* **2014**, *141* (4), 044314.
- (20) Eland, J. Photoelectron spectra of conjugated hydrocarbons and heteromolecules. *International Journal of Mass Spectrometry and Ion Physics* **1969**, 2 (6), 471–484.
- (21) Snellenburg, J. J.; Laptenok, S.; Seger, R.; Mullen, K. M.; van Stokkum, I. H. M. Glotaran: A *Java*-Based Graphical User Interface for the *R* Package TIMP. *Journal of Statistical Software* **2012**, 49 (3), 1–22.
- (22) Neese, F. The ORCA program system. Wiley Interdisciplinary Reviews: Computational Molecular Science 2012, 2 (1), 73–78.
- (23) El-Shahawy, A. S.; Hammam, A. S. CNDO/SCF molecular orbital structural studies and charge transfer complex formation between 4, 4'-dimethoxydiquinone and uracil. *Bull. Chem. Soc. Ethiop.* **2004**, *18* (2), 193–204.

- (24) Mayer, D.; Picconi, D.; Robinson, M. S.; Gühr, M. Experimental and theoretical gas-phase absorption spectra of thionated uracils. *Chem. Phys.* **2022**, *558*, 111500.
- (25) Mai, S.; Mohamadzade, A.; Marquetand, P.; González, L.; Ullrich, S. Simulated and experimental time-resolved photoelectron spectra of the intersystem crossing dynamics in 2-thiouracil. *Molecules* **2018**, 23 (11), 2836.

### **□** Recommended by ACS

Influence of a Methyl Group on the Unidirectional Flow of Vibrational Energy in an Adenine-Thymine Base Pair

H. K. Shin.

JANUARY 03, 2023

THE JOURNAL OF PHYSICAL CHEMISTRY B

READ 🗹

Vertical Excitation Energies and Lifetimes of the Two Lowest Singlet Excited States of Cytosine, 5-Aza-cytosine, and the Triazine Family: Quantum Mechanics—Molecula...

Ondřej Tichý, Jaroslav V. Burda, et al.

MARCH 24, 2023

JOURNAL OF CHEMICAL THEORY AND COMPUTATION

READ 🗹

## Triatomic Photoassociation in an Ultracold Atom-Molecule Collision

Ahmed A. Elkamshishy and Chris H. Greene

DECEMBER 30, 2022

THE JOURNAL OF PHYSICAL CHEMISTRY A

READ 🗹

#### Direct Observation of Excitation Wavelength-Dependent Ultrafast Intersystem Crossing in Cytosine Nucleoside Solution

Peicong Wu, Jinquan Chen, et al.

SEPTEMBER 30, 2022

THE JOURNAL OF PHYSICAL CHEMISTRY B

READ 🗹

Get More Suggestions >